Voltage tunable two-color infrared detection using semiconductor superlattices

Amlan Majumdar[a)]
Department of Electrical Engineering, Princeton University, Princeton, New Jersey 08544

K. K. Choi
U.S. Army Research Laboratory, Adelphi, Maryland 20783

J. L. Reno
Sandia National Laboratories, Albuquerque, New Mexico 87185

D. C. Tsui
Department of Electrical Engineering, Princeton University, Princeton, New Jersey 08544

(Received 27 August 2003; accepted 29 October 2003)

We demonstrate a voltage tunable two-color quantum-well infrared photodetector (QWIP) that consists of multiple periods of two distinct AlGaAs/GaAs superlattices separated by AlGaAs blocking barriers on one side and heavily doped GaAs layers on the other side. The detection peak switches from 9.5 μm under large positive bias to 6 μm under negative bias. The background-limited temperature is 55 K for 9.5 μm detection and 80 K for 6 μm detection. We also demonstrate that the corrugated-QWIP geometry is suitable for coupling normally incident light into the detector. © *2003 American Institute of Physics.* [DOI: 10.1063/1.1635981]

Voltage tunable two-color detectors are required for many applications of infrared detection, such as remote temperature sensing and chemical analysis. Quantum-well infrared photodetectors (QWIPs) with voltage tunable detection peaks have received a lot of attention as these two-terminal devices simplify the production of high-uniformity focal plane arrays (FPAs).[1] Voltage tunable QWIPs developed so far use Stark shift,[2] multiple transitions in heavily doped quantum wells (QWs),[3] multistack structures,[4] or electron transfer between coupled QWs.[5] These approaches have certain drawbacks, such as small tuning range,[2] low detectivity,[3] large temperature dependence,[4] and low operating temperature,[6] respectively. Dipole transitions between energy minibands in superlattices (SLs) have also been utilized for long-wavelength (LW)[7–9] and mid-wavelength (MW)[10] infrared detection. Two-color detection was recently demonstrated using a superlattice infrared photodetector (SLIP) consisting of two distinct SLs separated by a blocking barrier.[11] This structure utilizes the low resistance of SLs and the high resistance of the blocking barriers to avoid most of the above-mentioned problems. Unfortunately, this original design contains only a single SL for each color, which leads to low absorption at both wavelengths. In addition, two-color FPA fabrication necessitates broadband light coupling scheme for normal incidence absorption. One such scheme is the corrugated-QWIP (C-QWIP), which requires a thick active layer for large reflecting sidewalls.[12] Therefore, multiple units of the SL pairs are needed for constructing a sensitive C-QWIP. In this letter, we propose and demonstrate a multiple SL structure, whose units are separated by wide layers of heavily doped GaAs, and show that C-QWIPs are indeed capable of coupling wide range of wavelengths for two-color detection.

The multiple SL structure, whose single unit is sketched in Fig. 1(a), consists of four periods of SL pairs cladded by thick n^+-GaAs contact layers. Each SL pair comprises of a bottom SL (SL1) and a top SL (SL2) with an undoped 600 Å thick linearly graded $Al_xGa_{1-x}As$ barrier in the middle ($x = 0.22 \rightarrow 0.4$ along the growth direction). Each SL1/graded-barrier/SL2 unit is separated from the next unit by a 2000 Å n^+-GaAs layer that is uniformly doped with 1×10^{18} cm^{-3} Si donors. SL1 and SL2 are designed for 7–11 μm and 4–7 μm detection, respectively. We will refer to these two detection ranges as the LW and the MW range, respectively. SL1 contains four periods of 65 Å GaAs wells and 40 Å $Al_{0.27}Ga_{0.73}As$ barriers while SL2 consists of four periods of 40 Å GaAs wells and 30 Å $Al_{0.4}Ga_{0.6}As$ barriers. The middle 35 Å of the GaAs wells in SL1 and the entire 40 Å GaAs wells in SL2 are uniformly doped with 1×10^{18} cm^{-3} Si donors while the barriers in both the SLs are undoped. The whole structure was grown on a (100) semi-insulating GaAs substrate by molecular-beam epitaxy.

The calculated conduction band diagram and energy levels of one period of the SLIP device at zero bias are shown in Fig. 1(b). Both short-period SLs give rise to minibands M_1 and M_2 that each contain four energy levels, E_1 through E_4. For the nominal doping densities, all four levels in M_1 of SL1 and the first three levels in M_1 of SL2 are occupied. When infrared radiation is coupled into the detector, transitions from the occupied states in M_1 to the empty states in M_2 in both SLs give rise to infrared absorption. Transitions, such as, M_1-$E_1 \rightarrow M_2$-E_4 and M_1-$E_4 \rightarrow M_2$-E_1, carry most of the oscillator strength because they conserve momentum along the SL direction. Although stand-alone SLs absorb infrared radiation, their current levels do not change noticeably upon illumination because electrons are equally conducting in both M_1 and M_2 minibands. The introduction of the 600 Å thick graded AlGaAs barrier between SL1 and SL2 forbids

a)Electronic mail: majumdar@ee.princeton.edu

Report Documentation Page

Form Approved
OMB No. 0704-0188

1. REPORT DATE	2. REPORT TYPE	3. DATES COVERED
22 DEC 2003		**-**

4. TITLE AND SUBTITLE	5a. CONTRACT NUMBER
Voltage tunable two-color infrared detection using semiconductor superlattices	**F29601-02-C-0267**
	5b. GRANT NUMBER
	5c. PROGRAM ELEMENT NUMBER **62601F**

6. AUTHOR(S)	5d. PROJECT NUMBER
Amian Majumdar; K Choi; J. Reno; D Tsui	**4846**
	5e. TASK NUMBER **CR**
	5f. WORK UNIT NUMBER **A1**

7. PERFORMING ORGANIZATION NAME(S) AND ADDRESS(ES)	8. PERFORMING ORGANIZATION REPORT NUMBER
Department of Electrical Engineering,Princeton University,Princeton,NJ,08544	

9. SPONSORING/MONITORING AGENCY NAME(S) AND ADDRESS(ES)	10. SPONSOR/MONITOR'S ACRONYM(S)
	11. SPONSOR/MONITOR'S REPORT NUMBER(S)

12. DISTRIBUTION/AVAILABILITY STATEMENT
Approved for public release; distribution unlimited

13. SUPPLEMENTARY NOTES

14. ABSTRACT

We demonstrate a voltage tunable two-color quantum-well infrared photodetector (QWIP) that consists of multiple periods of two distinct AlGaAs/GaAs superlattices separated by AlGaAs blocking barriers on one side and heavily doped GaAs layers on the other side. The detection peak switches from 9.5 mu m under large positive bias to 6 mu m under negative bias. The background-limited temperature is 55 K for 9.5 mu m detection and 80 K for 6 mu m detection. We also demonstrate that the corrugated-QWIP geometry is suitable for coupling normally incident light into the detector.

15. SUBJECT TERMS

16. SECURITY CLASSIFICATION OF:			17. LIMITATION OF ABSTRACT	18. NUMBER OF PAGES	19a. NAME OF RESPONSIBLE PERSON
a. REPORT	b. ABSTRACT	c. THIS PAGE			
unclassified	**unclassified**	**unclassified**		**4**	

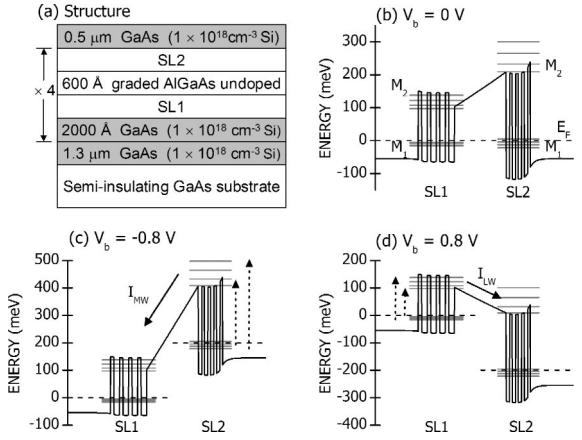

FIG. 1. (a) Layer structure of the two-color SLIP. The conduction-band diagram and energy levels of the SLIP at bias voltage $V_b=0$ V (b), -0.8 V (c), and 0.8 V (d). M_1 and M_2 are the first and second minibands and E_F is the Fermi level. The dashed arrows indicate the shortest and the longest possible miniband-to-miniband transitions in (c) SL2 that give rise to MW photocurrent I_{MW}, and (d) SL1 that produce LW photocurrent I_{LW}.

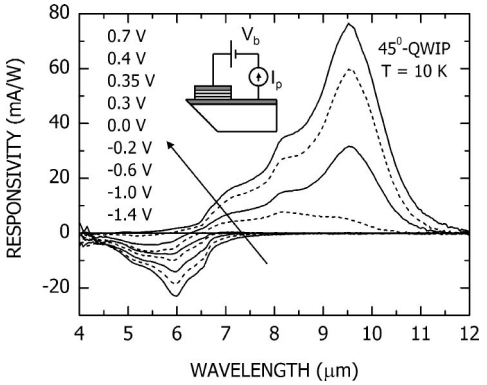

FIG. 2. Spectral responsivity R of 45°-edge coupled detectors at temperature $T=10$ K and bias voltage V_b in the range from 0.7 to -1.4 V (top to bottom curve). Alternate curves are shown with solid and dashed lines for clarity. Inset: Scheme for applying bias V_b to and measuring photocurrent I_p of an edge-coupled detector.

conduction via M_1 in one of the directions, and hence, leads to a photocurrent from the respective SLs. Under large positive bias applied to the top contact [Fig. 1(d)], the conduction of electrons in M_1 of SL1 is blocked, and hence, the increase in current flow through M_2 of SL1 in the presence of light produces a photocurrent. This situation is reversed under negative bias [Fig. 1(c)] with SL2 giving rise to a photocurrent. The different absorption wavelengths in the two SLs thus provide a physical mechanism for voltage tunable two-color detection with SL1 producing a LW photocurrent I_{LW} under large positive bias and SL2 a MW photocurrent I_{MW} under negative bias.

To build a multiple SL structure, it is important to realize that the conduction of M_1 electrons in SL1 under negative bias will eventually be blocked by the thick barrier at the next unit on the left-hand side in Fig. 1(c). If the LW photoelectrons from SL1 are able to pass through that thick barrier, they will create I_{LW} in the next stage, which is in addition to I_{MW} in the present stage due to SL2. Both wavelengths will then be detected under the same bias, which is undesirable for the present application. The above-described situation also applies to SL2 under positive bias. Therefore, it is important to isolate the transport of photoelectrons, which are high-energy electrons, between adjacent units. To achieve this goal, a 2000 Å wide n^+-GaAs region is inserted between the units as a hot-electron blocking layer.[13,14] With this layer, the LW photoelectrons under negative bias lose all their energy before reaching the next unit, and hence, will not give rise to I_{LW}. The same is true for MW photoelectrons under positive bias. From this discussion, it is clear that the present detector relies on two types of blocking layers to achieve voltage tunable operation: A thick barrier for low-energy electrons and a thick doped layer for high-energy electrons.

We now present results from 45°-edge coupled devices that were processed for standard detector characterization. Spectral responsivity R of these detectors was measured in the 10–65 and 10–100 K temperature ranges for positive and negative bias, respectively. As sketched in the inset of Fig. 2, we apply bias voltage V_b to the top contact while keeping the bottom one grounded and measure photocurrent using standard ac lock-in techniques. A plot of R of a typical detector at temperature $T=10$ K is shown in Fig. 2. As expected, LW photoresponse is observed under large positive bias while MW response is observed under negative bias.

For positive bias $V_b>0.35$ V, the LW response is broad and is peaked at $\lambda_p=9.5$ μm with a 10.3 μm cutoff wavelength. In addition, two shoulders are observed at 7.15 and 8.2 μm. These three peaks are due to the M_1-$E_1\rightarrow M_2$-E_4, M_1-$E_2\rightarrow M_2$-E_3, and M_1-$E_3\rightarrow M_2$-E_2 transitions in SL1. The absence of a fourth peak expected at $\sim$10.5 μm indicates that the energy level M_1-E_4 is empty, which we attribute to lower effective doping in SL2 than the intended value.[15] At lower bias, the LW response peak shifts to shorter wavelengths, first to $\lambda_p=8.2$ μm and then to $\lambda_p=7.15$ μm. The wavelength shift is due to the higher effective barrier height at the tip of the graded barrier at lower bias. The existence of a build-in field at the graded barrier also creates a MW photovoltaic response between 0 and 0.4 V, leading to the observation of both wavelengths within this bias range. This observation is in agreement with the expected value of $V_b=0.42$ V when the electric field in the graded barrier reverses direction. The LW response has negligible T dependence and decreases by $\sim$5% as T is raised from 10 to 65 K.

The MW response is peaked at $\lambda_p=6$ μm under negative bias and vanishes for $V_b>0.5$ V, which is consistent with the calculated energy level structure. The spectra are broad with spectral width $\Delta\lambda=1.6$ μm ($\Delta\lambda/\lambda_p\sim 25\%$). The MW response exhibits negligible T dependence up to 100 K. It is clear from Fig. 2 that the MW response is smaller than the LW response. The ratio of the peak LW and MW responsivity is $R(\lambda=9.5\ \mu\mathrm{m}, V_b=0.7\ \mathrm{V})/R(\lambda=6\ \mu\mathrm{m}, V_b=-1.0\ \mathrm{V})=3.7$. One should note that R is inversely proportional to the square of the transition energy, and hence, directly proportional to λ^2. The dipole matrix elements of SL1 and SL2 are very similar, and therefore, R in the LW range should be 2.5 times larger than that in the MW range. The observed factor of 3.7 can be attributed to the larger LW photoconductive gain. Therefore, the smaller MW response found in Fig. 2 is expected in our detector structure.

We measured detector dark current I_d from $T=4.2$ to

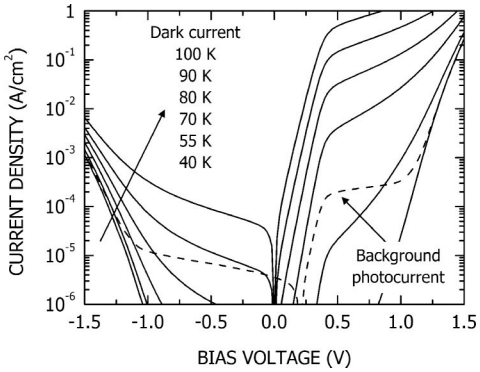

FIG. 3. Bias dependence of dark current (solid lines) and background photocurrent (dashed lines) density of the two-color SLIP. The temperature $T=100$, 90, 80, 70, 55, and 40 K (top to bottom) for the dark current curves while $T=10$ K for the background photocurrent curve.

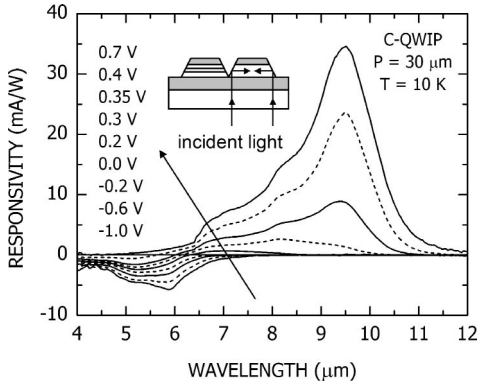

FIG. 4. Spectral responsivity R of a C-QWIP with corrugation period $P=30$ μm at temperature $T=10$ K and bias voltage V_b in the range from 0.7 to -1.0 V (top to bottom curve). Alternate curves are plotted with solid and dashed lines for clarity. Inset: Cross-sectional view of a C-QWIP.

200 K. Some of these dark current–voltage curves are plotted in Fig. 3 along with the window current I_w that was generated by 300 K background radiation. The window current measurement was carried out with the detector temperature fixed at $T=10$ K and the background radiation incident through $F/1.2$ optics. We define the background-limited temperature T_{BLIP} as the temperature when $I_d=I_w$.[1] From Fig. 3, we determined that $T_{\mathrm{BLIP}}=55$ K for $0<V_b\leqslant 0.8$ V for LW detection and 80 K for $-0.8\leqslant V_b\leqslant 0$ V for MW detection. These values of T_{BLIP} are comparable to those of one-color detectors with similar cutoff wavelengths.[1] We also extracted electron activation energy E_a from the T dependence of I_d and found that these values are consistent with the band diagram sketched in Fig. 1. For instance, the deduced value of $E_a=175$ meV as $V_b\rightarrow 0$ V is in good agreement with the expected value of $E_a=185$ meV at $V_b=0$ V.

We processed C-QWIPs to demonstrate normal-incidence photoresponse, which is necessary for FPA fabrication.[12] In the C-QWIP geometry [see inset of Fig. 4], light is normally incident on the back side of the wafer, suffers total internal reflection at the etched sidewalls, and then, travels parallel to the QWs, leading to intersubband absorption. We plot R of a C-QWIP with corrugation period $P=30$ μm at $T=10$ K in Fig. 4. The peak positions of the C-QWIP spectra are similar to those of the edge-coupled detector. However, with respect to the LW response, the MW response of the C-QWIP is smaller than that of the edge-coupled detector. The ratio $R(\lambda=9.5\ \mu\mathrm{m}, V_b=0.7\ \mathrm{V})/R(\lambda=6\ \mu\mathrm{m}, V_b=-1.0\ \mathrm{V})$ is now equal to 6 instead of 3.7 for the edge-coupled detector. This difference needs further investigation. In addition, R of the C-QWIP is smaller than that of the edge-coupled detector. It is due to the fact that the present C-QWIP is a relatively flat trapezoid with a base width of 30 μm and an active thickness height of 1.32 μm. The projected reflecting surface is therefore very small. R is expected to increase if thicker active material or other high gain materials, such as InGaAs/GaAs, are used.

In conclusion, we have demonstrated a voltage tunable two-color detector that contains multiple periods of AlGaAs/GaAs superlattice pairs. The peak wavelength switches from 9.5 μm under large positive bias to 6 μm under negative bias. The background-limited temperature is 55 K for 9.5 μm detection and 80 K for 6 μm detection. We have also demonstrated that C-QWIPs are capable of coupling normally incident light for this two-color application. Using different SL pairs, one should be able to achieve different two-color combinations, such as, MW/LW, MW/MW, LW/LW, and LW/very LW. Their bandwidths can also be individually adjusted to suit a specific application. Therefore, we have demonstrated a highly versatile two-color detection scheme for large format FPAs.

The work at Princeton University is supported by grants from the Army Research Office and the Air Force Research Laboratory (Kirtland). Sandia is a multiprogram laboratory operated by Sandia Corporation, a Lockheed–Martin Company, for the United States Department of Energy under Contract No. DE-AC04-94AL85000.

[1] K. K. Choi, *The Physics of Quantum Well Infrared Photodetectors* (World Scientific, River Edge, New Jersey, 1997).
[2] S. R. Parihar, S. A. Lyon, M. Santos, and M. Shayegan, Appl. Phys. Lett. **55**, 2417 (1989).
[3] K. Kheng, M. Ramsteiner, H. Schneider, J. D. Ralston, F. Fuchs, and P. Koidl, Appl. Phys. Lett. **61**, 666 (1992).
[4] H. C. Liu, J. Li, J. R. Thompson, Z. R. Wasilewski, M. Buchanan, and J. G. Simmons, IEEE Electron Device Lett. **14**, 566 (1993).
[5] A. Majumdar, K. K. Choi, J. L. Reno, L. P. Rokhinson, and D. C. Tsui, Appl. Phys. Lett. **80**, 707 (2002).
[6] A. Majumdar, K. K. Choi, J. L. Reno, L. P. Rokhinson, and D. C. Tsui, Appl. Phys. Lett. **82**, 686 (2003).
[7] A. Kastalsky, T. Duffield, S. J. Allen, and J. Harbison, Appl. Phys. Lett. **52**, 1320 (1988).
[8] S. D. Gunapala, B. F. Levine, and N. Chand, J. Appl. Phys. **70**, 305 (1991).
[9] K. M. S. V. Bandara, J. W. Choe, M. H. Francombe, A. G. U. Perera, and Y. F. Lin, Appl. Phys. Lett. **60**, 3022 (1992).
[10] K. K. Choi, S. V. Bandara, S. D. Gunapala, W. K. Liu, and J. M. Fastenau, J. Appl. Phys. **91**, 551 (2002).
[11] C. C. Chen, H. C. Chen, C. H. Kuan, S. D. Lin, and C. P. Lee, Appl. Phys. Lett. **80**, 2251 (2002).
[12] C. J. Chen, K. K. Choi, M. Z. Tidrow, and D. C. Tsui, Appl. Phys. Lett. **68**, 1446 (1996).
[13] J. R. Hayes, A. F. J. Levi, and W. Wiegmann, Phys. Rev. Lett. **54**, 1570 (1985).
[14] M. Heiblum, M. I. Nathan, D. C. Thomas, and C. M. Knoedler, Phys. Rev. Lett. **55**, 2200 (1985).
[15] A. R. Ellis, A. Majumdar, K. K. Choi, J. L. Reno, and D. C. Tsui (unpublished).